

Differential Protein Mobility of the γ -Aminobutyric Acid, Type A, Receptor α and β Subunit Channel-lining Segments*

Received for publication, September 21, 2004, and in revised form, October 29, 2004
Published, JBC Papers in Press, November 2, 2004, DOI 10.1074/jbc.M410881200

Jeffrey Horenstein, Paul Riegelhaupt, and Myles H. Akabas \ddagger

From the Departments of Physiology and Biophysics and of Neuroscience, Albert Einstein College of Medicine, Yeshiva University, Bronx, New York 10461

The γ -aminobutyric acid, type A (GABA_A), receptor ion channel is lined by the second membrane-spanning (M2) segments from each of five homologous subunits that assemble to form the receptor. Gating presumably involves movement of the M2 segments. We assayed protein mobility near the M2 segment extracellular ends by measuring the ability of engineered cysteines to form disulfide bonds and high affinity Zn²⁺-binding sites. Disulfide bonds formed in $\alpha_1\beta_1$ E270C γ_2 but not in α_1 N275C $\beta_1\gamma_2$ or $\alpha_1\beta_1\gamma_2$ K285C. Diazepam potentiation and Zn²⁺ inhibition demonstrated that expressed receptors contained a γ subunit. Therefore, the disulfide bond in $\alpha_1\beta_1$ E270C γ_2 formed between non-adjacent subunits. In the homologous acetylcholine receptor 4-Å resolution structure, the distance between α carbon atoms of 20' aligned positions in non-adjacent subunits is ~19 Å. Because disulfide trapping involves covalent bond formation, it indicates the extent of movement but does not provide an indication of the energetics of protein deformation. Pairs of cysteines can form high affinity Zn²⁺-binding sites whose affinity depends on the energetics of forming a bidentate-binding site. The Zn²⁺ inhibition IC₅₀ for $\alpha_1\beta_1$ E270C γ_2 was 34 nM. In contrast, it was greater than 100 μ M in α_1 N275C $\beta_1\gamma_2$ and $\alpha_1\beta_1\gamma_2$ K285C receptors. The high Zn²⁺ affinity in $\alpha_1\beta_1$ E270C γ_2 implies that this region in the β subunit has a high protein mobility with a low energy barrier to translational motions that bring the positions into close proximity. The differential mobility of the extracellular ends of the β and α M2 segments may have important implications for GABA-induced conformational changes during channel gating.

GABA_A¹ receptors are allosteric proteins that mediate fast inhibitory neurotransmission in the central nervous system (1–3). They are members of the Cys-loop receptor ion channel gene superfamily that includes glycine, serotonin type 3 (5-HT₃), and nicotinic acetylcholine (ACh) receptors (4–6). GABA_A receptors are formed by five homologous subunits as-

sembled around a central channel. Most endogenous receptors contain two α , two β , and one γ subunit arranged in a clockwise orientation $\alpha\beta\alpha\beta\gamma$ when observed from the extracellular end of the channel (7, 8). However, expression of just α and β subunits also results in functional receptors with the favored stoichiometry being two α and three β in the order $\alpha\beta\alpha\beta\beta$ (9–11). Each subunit has an ~200-amino acid, extracellular, N-terminal, ligand-binding domain and a C-terminal, channel-forming domain with four membrane-spanning segments (M1, M2, M3, and M4).

The channel is principally lined by the five α -helical M2 segments (12, 13). An index numbering system facilitates comparisons between M2 segments of superfamily members (14). The 0' position is defined as the positively charged residue located near the cytoplasmic end of the channel, GABA_A β_1 R250. The 20' position, GABA_A β_1 E270, is aligned with the acetylcholine receptor extracellular ring of charge (15) and is predicted by amino acid sequence analysis to be the extracellular end of M2 (16). Experimental evidence indicates that M2 extends two helical turns beyond the 20' position (17). The 4-Å resolution structure of the homologous *Torpedo* ACh receptor confirms this and demonstrates that the 20' position lies at the level of the extracellular membrane surface (13). In the 4-Å resolution cryo-EM structure the narrowest region of the closed channel, inferred to be the gate, is near the midpoint, between the 9' and 14' positions (13). Cysteine accessibility studies in the 5-HT₃ receptor are consistent with this, although similar studies in the ACh receptor concluded that the gate was at the channel's cytoplasmic end (18, 19). Evidence from ACh, GABA_A, and 5-HT₃ receptors indicates that the structure of the cytoplasmic end of the channel is relatively fixed and rigid (20–22). This would be consistent with evidence that the size and charge selectivity filters, and the major determinants of single channel conductance are located at the cytoplasmic end of the channel (12, 15, 23–25). In contrast, the extracellular end of the channel undergoes conformational motion due to both thermal protein motion and agonist-induced gating (17, 20, 21, 26). In the cryo-EM-derived structure, the extracellular ends of the M2 domains are loosely packed, suggesting that these domains might possess a high degree of flexibility/mobility (13). Consistent with this, substituted cysteine accessibility method studies of the GABA_A receptor β_1 subunit M2 domain concluded that the M2 segment extracellular halves were loosely packed and/or highly mobile (21).

We previously used disulfide trapping experiments in $\alpha\beta$ receptors to probe thermal protein motion and proximity relationships between M2 segment, channel-lining residues in different subunits (26). The ability for a pair of cysteines to form a disulfide bond depends on the presence of an oxidizing environment and on the collision frequency. The collision frequency depends on the average separation distance of the sulfhydryls, their relative orientation in the protein, and the flexibility/

* This work was supported by National Institutes of Health Grants NS30808 and GM61925 (to M. H. A.). The costs of publication of this article were defrayed in part by the payment of page charges. This article must therefore be hereby marked "advertisement" in accordance with 18 U.S.C. Section 1734 solely to indicate this fact.

\ddagger To whom correspondence should be addressed: Dept. of Physiology & Biophysics, Albert Einstein College of Medicine, 1300 Morris Park Ave., Bronx, NY 10461. Tel.: 718-430-3360; Fax: 718-430-8819; E-mail: makabas@aecom.yu.edu.

¹ The abbreviations used are: GABA_A, γ -aminobutyric acid, type A; ACh, acetylcholine; cryo-EM, cryoelectron-microscopy; Cu:phen, copper phenanthroline; DTT, dithiothreitol; CFFR, calcium-free frog Ringer's solution; 5-HT₃, 5-hydroxytryptamine type 3; NEM, N-ethylmaleimide; Tricine, N-[2-hydroxy-1,1-bis(hydroxymethyl)-ethyl]glycine.

mobility of the protein in the region of the Cys residues. We used copper phenanthroline (Cu:phen) to create an oxidizing environment. Cu:phen catalyzes the formation of reactive oxygen species, such as superoxide and hydroxyl radicals, from molecular oxygen (27). We showed that at the 20' level disulfide bonds formed between Cys substituted for the β 20' but not between Cys substituted for the α 20'. In order for a disulfide bond to form, the Cys α carbons must come to within 5.6 Å of one another (28). Assuming that the 4-Å resolution ACh receptor structure is a good model for the GABA_A receptor structure, the average distance between the 20' α carbons of residues in adjacent and non-adjacent subunits is 12 and 19 Å, respectively (13). Because there are three β subunits in the $\alpha\beta$ receptors used in our previous work, we could not distinguish whether the disulfide bond was forming between Cys substituted in adjacent or in non-adjacent positions. Thus, the extent of the thermal motion could not be determined (26). To resolve this issue the current experiments have been performed in $\alpha\beta\gamma$ receptors where the two β subunits are not adjacent.

The extent of the movements that would be required to explain the disulfide bond formation in our original studies highlights a potential limitation of disulfide trapping experiments. Because disulfide bonds are covalent they may trap relatively rare conformational states of the protein. In the aspartate chemotaxis receptor, a protein of known crystal structure, thermal protein movement allowed disulfide bond formation between pairs of engineered Cys whose α carbons were separated in the crystal structure by 15 Å (28). Thus, disulfide trapping may provide insight into the extent of thermal motion, but it does not necessarily measure the average separation distances. To address this issue, in the present work we have measured the Zn²⁺ binding affinity of receptors containing pairs of engineered Cys. Pairs of Cys can form bidentate, high affinity Zn²⁺-binding sites if they are positioned appropriately. The Zn²⁺ affinity of these sites will depend on the orientation of the Cys sulfur atoms, their average separation distance, and the energy needed to distort the average protein structure to bring the Cys into position to bind the Zn²⁺ ion. The Zn²⁺ affinity will lie between the picomolar range, the affinity of Zn²⁺ for peptides containing four Cys Zn²⁺ finger-binding protein sequences (29), and the 10–1000 μ M range, the Zn²⁺ affinity of single Cys (10, 30, 31). In crystal structures of high affinity Zn²⁺-binding sites the Cys α carbons are separated by about 5–7 Å. The non-covalent nature of this interaction provides a better estimate of the average separation and/or the energy required to distort the average conformation to the structure necessary for high affinity binding.

Disulfide trapping has been used to study protein mobility and proximity relationships between residues in both water-soluble and integral-membrane proteins (28, 32–34). Engineering heavy metal-binding sites has been used to study proximity relationships in ion channels and transporters (10, 35–37).

Here we report that in $\alpha\beta\gamma$ receptors disulfide bonds form when all five subunits contain 20' engineered Cys residues, but for the single Cys mutants they only form when the engineered Cys is in the β subunit, not when it is in α or γ . Consistent with this, a high affinity Zn²⁺-binding site is only formed when the engineered Cys is in the β subunit. These results provide insights into the extent and asymmetric nature of the thermal motion near the extracellular ends of the GABA_A receptor channel-lining M2 segments and have implications for the channel gating process.

EXPERIMENTAL PROCEDURES

Mutagenesis and Oocyte Expression—All cysteine substitution mutants were made using PCR as described previously (21). mRNA was synthesized *in vitro* using the Amplicap T7 High Yield Message Maker

kit (Epicenter Technologies, Madison, WI). mRNA was dissolved in diethylpyrocarbamate-treated water and stored at –80 °C. *Xenopus laevis* were purchased from Nasco Science (Fort Atkinson, WI). Stage V–VI oocytes were defolliculated by incubation in 2 mg/ml Type 1A collagenase (Sigma) for 75 min. Oocytes were washed in OR2 (82.5 mM NaCl, 2 mM KCl, 1 mM MgCl₂, 5 mM HEPES; pH adjusted to 7.5 with NaOH) and kept in OR3 (70% Leibovitz L-15 medium (Invitrogen) supplemented with 10 mM HEPES, 50 μ g/ml tetracycline, and 50 μ g/ml gentamicin). Oocytes were injected 24 h after isolation with 50 nl of a 1:1:1 mixture of rat $\alpha_1\beta_1\gamma_{2S}$ subunit mRNA (200 pg/ml) and were kept in OR3 medium for 2–5 days at 17 °C.

Reagents—A 100 mM stock solution of GABA (Sigma) in water was aliquoted and stored at –20 °C. 1 M stock solutions of dithiothreitol (DTT; Sigma) and *o*-phenanthroline (Sigma) were made in nominally calcium-free frog Ringer's solution (CFFR: 115 mM NaCl, 2.5 mM KCl, 1.8 mM MgCl₂, and 10 mM HEPES, pH 7.5) and Me₂SO, respectively, aliquoted, and stored for not more than 1 month at –20 °C. A stock solution of 100 mM CuSO₄ was made in water. CuSO₄ and *o*-phenanthroline were mixed in CFFR directly before use to a final concentration of 100 μ M CuSO₄ and 400 μ M *o*-phenanthroline, expressed as 100:400 μ M Cu:phen. A 100 mM stock solution of *N*-ethylmaleimide (NEM, Sigma) was made in CFFR directly before use. A 10 mM diazepam stock solution was made in Me₂SO and stored at –20 °C. A 100 mM ZnCl₂ (Sigma) stock solution was made in water with 10 mM HCl, to prevent the precipitation of Zn²⁺ (OH[–]). Tricine (Sigma) was diluted directly into 1× buffer at a concentration on 10 mM. Stock solutions of 500 mM *N*-(2-acetamido)iminodiacetic acid (Sigma), pH 7.3, and 100 mM diethylenetriaminepentaacetic acid (Sigma), pH 7.3, were made in water.

Electrophysiology—Two-electrode voltage clamp recordings were conducted at room temperature in a 250- μ l chamber continuously perfused at 5–6 ml/min with CFFR solution. For the Zn²⁺ dose-response curves, CFFR was replaced by a buffer containing 100 mM NaCl, 2.8 mM KCl, 0.3 mM BaCl₂, and 5 mM HEPES, pH 7.3. Currents were recorded from oocytes using two-electrode voltage clamp recording at a holding potential of –60 mV. The ground electrode was connected to the bath via a 3 M KCl/Agar bridge. Glass microelectrodes filled with 3 M KCl had a resistance of <2 M Ω . Data were acquired and analyzed using a TEV-200 amplifier (Dagan Instruments, Minneapolis, MN), a Digidata 1322A data interface (Axon Instruments, Union City, CA), and pClamp 8 software (Axon Instruments). Currents were elicited by applications of GABA separated by at least 5 min of CFFR wash to allow complete recovery from desensitization. Currents were judged to be stable if the variation between consecutive GABA pulses was <5%.

Diazepam-induced Current Enhancement—The GABA dose-response relationship was determined on each cell. A GABA EC₅ concentration was applied in the absence and presence of 1 μ M diazepam. To prevent disulfide bond formation receptors were kept reduced by the application of 10 mM DTT at the beginning of the experiment and between pulses of reagents. The amount of potentiation by diazepam was calculated by the equation, % potentiation = (I_{Dzpm}/I) \times 100, where I_{Dzpm} and I are the GABA-induced currents with and without diazepam, respectively. The diazepam potentiation is presented as the mean \pm S.E.

NEM Inhibition of Zn²⁺ Binding—After a control pulse of 30 μ M GABA, 5 μ M Zn²⁺ was applied for 1 min, followed by co-application of GABA and Zn²⁺. To eliminate Zn²⁺ binding to the engineered cysteines, receptors were treated with 100 μ M NEM for 5 min. We then reapplied GABA, first alone and then in the presence of Zn²⁺. (In some cases the effect of NEM on Zn²⁺-induced inhibition was tested on separate cells. Because this did not alter the outcome, the results of all experiments were combined.) Receptors were kept reduced by the application of 10 mM DTT at the beginning of the experiments and between pulses of reagents. Prior to every pulse of GABA or GABA plus Zn²⁺, receptors were reduced with DTT (10 mM, 5–10 min) and either washed (GABA pulses) or treated with Zn²⁺ (GABA plus Zn²⁺ pulses) for 1 min. The degree of inhibition by Zn²⁺ both before and after NEM treatment was determined by the equation, % inhibition = [1 – (I_{zn}/I)] \times 100, where I_{zn} and I are the GABA-induced currents with and without Zn²⁺, respectively. The % inhibition is given as mean \pm S.E.

Disulfide Bond-induced Inhibition—Once GABA-induced control currents had stabilized, 10 mM DTT was applied for 10 min. GABA was reapplied directly following DTT to determine the extent of potentiation produced by reduction of spontaneously formed disulfide bonds. The cells were treated with 100:400 μ M Cu:phen for 3–6 min, and then two or more GABA test pulses were applied. A second application of DTT was followed by a final pulse of GABA, to assure the reversibility of the Cu:phen effects.

Intersubunit disulfide bond formation was completely spontaneous and did not require catalysis by Cu:phen. Cu:phen only increased the

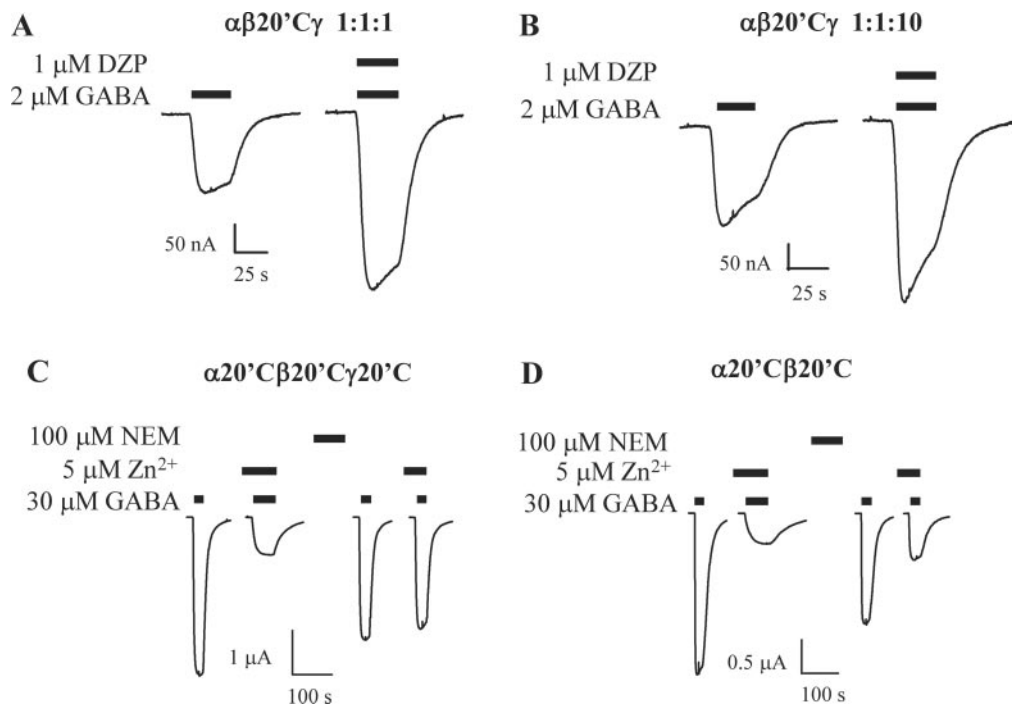


FIG. 1. Functional receptors contain a γ subunit. *A* and *B*, injection of a 1:1:1 molar ratio of α : β : γ mRNA gives full incorporation of the γ subunit. Receptors were kept reduced by applications of 10 mM DTT throughout the experiments. Diazepam-induced potentiation of oocytes injected with 1:1:1 (*A*) and 1:1:10 (*B*) molar ratios of α : β : γ mRNA. In the experiments shown, 1 μ M diazepam potentiated currents induced by 2 μ M GABA by 126% (1:1:1) and 94% (1:1:10). *C* and *D*, cells injected with $\alpha 20' C \beta 20' C \gamma 20' C$ are unaffected by 5 μ M Zn^{2+} following alkylation of engineered cysteines. The ability of 5 μ M Zn^{2+} to inhibit currents in cells injected with $\alpha 20' C \beta 20' C \gamma 20' C$ (*C*) and $\alpha 20' C \beta 20' C$ (*D*) mRNA was tested before and after treatment with 100 μ M NEM (5 min). Zn^{2+} inhibition was nearly abolished by NEM in $\alpha 20' C \beta 20' C \gamma 20' C$, but not $\alpha 20' C \beta 20' C$, proving that a γ subunit was present in receptors injected with $\gamma 20' C$ mRNA. Bars above traces indicate application of reagent. Leak currents have been subtracted. Current is not shown during application of Zn^{2+} alone or NEM. Holding potential: -60 mV.

rate of disulfide bond formation. Therefore, the extent of inhibition attributed to the presence of disulfide bonds was calculated by the equation, % inhibition = $[(I_{DTT} - I)/I_{DTT}] \times 100$, where I_{DTT} is the GABA-induced current following application of DTT, and I is the current prior to DTT treatment. A saturating concentration of GABA was used for all experiments, except where specified. The range of GABA concentrations was between 0.3 and 10 mM. The maximal currents and % effect for each reagent are presented as the mean \pm S.E.

Reoxidation Rates—A control pulse of a low concentration of GABA (below the GABA EC_{50}) was followed by a 10-min application of 10 mM DTT. This led to an increase in the size of the currents. Pulses of GABA were then applied at 5- to 10-min intervals to monitor the return of the currents to their unreduced levels. The peak currents were fit with the equation, $I_t = (I_0 - I_\infty) \exp(-t/\tau) + I_\infty$, where I_t is the current at time t , I_0 is the initial current, I_∞ is the final current, and τ is the time at which 63% of the total current decay occurred.

Zn^{2+} Dose-response Curves—A control pulse of GABA was followed by coapplications of GABA with increasing concentrations of Zn^{2+} . Prior to every pulse of GABA or GABA plus Zn^{2+} , receptors were reduced with DTT (10 mM, 5–10 min) and either washed or treated with Zn^{2+} for 1 min. Currents were normalized to the initial, control current, and fit with the Hill equation, $I/I_{max} = 1/[1 + (IC_{50}/Zn)^n]$, where I is the current, I_{max} is the control current, IC_{50} is the Zn^{2+} concentration that produces half-maximal inhibition, Zn is the Zn^{2+} concentration, and n is the Hill coefficient. Fits were performed in Prism 3.02 (GraphPad Software, San Diego, CA).

To avoid artifacts caused by potential submicromolar levels of heavy metal contamination, Zn^{2+} dose-response curves were performed in the presence of heavy metal chelators as described (38, 39). 10 mM Tricine was present in all solutions in which the final Zn^{2+} concentrations were in the range of 1 nM to 1 μ M. Under these conditions, $[Free\ Zn^{2+}]$ was equal to $[Added\ Zn^{2+}]/200$. 1 mM *N*-(2-acetamido)iminodiacetic acid was added to all Zn^{2+} -containing solutions in which the final Zn^{2+} concentrations were <1 nM. Under these conditions, $[Free\ Zn^{2+}]$ was equal to $[Added\ Zn^{2+}]/17,000$. Solutions requiring a final Zn^{2+} concentration of greater than 1 μ M had no chelator added. To solutions requiring no free Zn^{2+} , the high affinity chelator diethylenetriaminepentaacetic acid was added to a concentration of 10 μ M. A concentration of 20–30 μ M GABA was used in all experiments. Tricine, *N*-(2-acetamido)iminodiacetic acid and diethylenetriaminepentaacetic acid had no significant effects on

control GABA-induced currents (data not shown). The relationship between free Zn^{2+} and added Zn^{2+} was determined by the chemical speciation program, Geochem.

Statistics—All statistical analyses were performed in Prism 3.02 using a one-way analysis of variance followed by the Newman-Keuls multiple comparison test.

RESULTS

A γ Subunit Is Present in Functional Receptors—In $\alpha\beta\gamma$ receptors β subunits are found only in non-adjacent positions, whereas in $\alpha\beta$ receptors there is a pair of β subunits in adjacent positions (see the introduction). Therefore, if a disulfide bond formed between β subunits, we could only know that this bond occurred between non-adjacent subunits if we also knew that a γ subunit was present in the receptor. We tested for the presence of a γ subunit using two approaches, diazepam potentiation and Zn^{2+} inhibition. In $\alpha\beta\gamma$ receptors, 1 μ M diazepam is reported to potentiate currents induced by an EC_5 concentration of GABA by more than 100%, whereas $\alpha\beta$ receptors are unaffected by diazepam (40, 41). Zn^{2+} also enables us to distinguish between $\alpha\beta$ and $\alpha\beta\gamma$ receptors, because $\alpha\beta$ receptors have a Zn^{2+} IC_{50} of ~ 0.5 μ M, whereas $\alpha_1\beta_1\gamma_2$ receptors are insensitive to Zn^{2+} (42, 10). The high affinity Zn^{2+} -binding site is formed in $\alpha\beta$ receptors by the β_1 His-267 (M2 17') in the adjacent β subunits. In $\alpha\beta\gamma$ receptors there are no adjacent β subunits and therefore no high affinity Zn^{2+} -binding site.

We tested the effects of diazepam on two populations of the mutant $\alpha\beta 20' C \gamma$ receptors. Half of the cells were injected with a 1:1:1 and half with a 1:1:10 molar ratio of α , β , and γ mRNA. If the cells injected with a 1:1:1 ratio of mRNA expressed the γ subunit in all cell surface receptors, then there should be no increase in the amount of diazepam potentiation in the cells injected with 1:1:10 compared with 1:1:1. To assure that the presence of spontaneously formed disulfide bonds did not interfere with the effects of diazepam and Zn^{2+} , the reducing

agent DTT was applied for several minutes before the application of all reagents. As seen in Fig. 1 (A and B), the degree of diazepam-induced potentiation in the two populations of receptors was not significantly different (1:1:1, $179 \pm 70\%$ ($n = 3$); 1:1:10, $108 \pm 18\%$ ($n = 3$)). Therefore, in our hands, the majority of the GABA-induced current from oocytes injected with an equimolar ratio of the three subunits arises from receptors containing a γ subunit. Similar results were obtained with other Cys mutant receptors used in this study.

To further support the conclusion that the functional cell surface receptors used in this study contained a γ subunit, we examined the extent of inhibition by Zn^{2+} . Two different mutants were used for the experiments with Zn^{2+} : the double Cys mutant, $\alpha 20'C\beta 20'C$, and the triple Cys mutant, $\alpha 20'C\beta 20'C\gamma 20'C$. In both cases we injected equimolar amounts of mRNA for each subunit. $5 \mu M$ Zn^{2+} should inhibit more than 50% of the current in the $\alpha 20'C\beta 20'C$ mutant while having no effect on the current of the $\alpha 20'C\beta 20'C\gamma 20'C$ mutant. Surprisingly, the two mutants showed similar amounts of Zn^{2+} -induced inhibition: $85 \pm 4\%$ ($n = 2$) and $69 \pm 8\%$ ($n = 5$) for $\alpha 20'C\beta 20'C$ and $\alpha 20'C\beta 20'C\gamma 20'C$, respectively (Fig. 1, C and D). Because the engineered cysteines in these mutants could potentially bind Zn^{2+} , we retested the effects of Zn^{2+} after exposing the reduced receptors to the alkylating agent NEM ($100 \mu M$, 5 min). Alkylation should abolish the ability of cysteine to bind heavy metals. NEM diminished currents in both mutants. However, following alkylation with NEM, $5 \mu M$ Zn^{2+} inhibited the remaining currents in $\alpha 20'C\beta 20'C$ and $\alpha 20'C\beta 20'C\gamma 20'C$ by $60 \pm 2\%$ ($n = 3$) and $6 \pm 2\%$ ($n = 4$), respectively. Therefore, we infer that double mutant $\alpha 20'C\beta 20'C$ cells retained a high affinity for Zn^{2+} following alkylation, because the native high affinity, Zn^{2+} -binding site composed of β_1 His-267 (17') in adjacent β subunits (42, 10) are insensitive to NEM. In contrast, in the triple mutant, $\alpha 20'C\beta 20'C\gamma 20'C$, after NEM alkylation Zn^{2+} no longer inhibited significantly, because in the presence of the γ subunit there are not adjacent β subunits to form a high affinity Zn^{2+} -binding site. The overall conclusion from the experiments with Zn^{2+} and diazepam is that, when injected with a 1:1:1 ratio of α , β , and γ mRNA, the large majority of cell surface receptors contain a γ subunit. The important implication of this finding for the experiments described below is that two α subunits are not in adjacent positions nor are the two β subunits.

Intersubunit Disulfide Bonds Form in the 20' Cysteine Mutants—In response to the initial GABA applications, cells expressing $\alpha 20'C\beta 20'C\gamma 20'C$ receptors, which contain engineered Cys in all five subunits, had maximal GABA-induced currents (I_{max}) of 457 ± 81 nA ($n = 11$) that were much smaller than those of wild-type, 3058 ± 405 nA ($n = 5$) (Fig. 2A, 2B, and 3A). Following application of DTT (10 mM, 10 min) the I_{max} for the wild-type receptors was unchanged (3221 ± 386 nA ($n = 5$)), whereas that of the mutant receptor increased nearly 10-fold ($\alpha 20'C\beta 20'C\gamma 20'C$: 4297 ± 320 nA ($n = 11$)). Therefore, we infer that DTT reduced intersubunit disulfide bonds that formed spontaneously in $\alpha 20'C\beta 20'C\gamma 20'C$.

We next determined whether the oxidizing agent Cu:phen, which catalyzes disulfide bond formation, could reverse the effects of DTT in $\alpha 20'C\beta 20'C\gamma 20'C$. A 3-min application of $100:400 \mu M$ Cu:phen decreased the $\alpha 20'C\beta 20'C\gamma 20'C$ currents by $89 \pm 12\%$ ($n = 3$). This was not significantly different than their initial levels. In contrast, a similar Cu:phen application had no effect on wild-type currents ($n = 3$) (Fig. 2, A and B). A subsequent DTT application restored the mutant receptor currents to within $5 \pm 2\%$ ($n = 3$) of the levels produced by the first DTT application.

To ensure that the effect of DTT was not due to chelation of

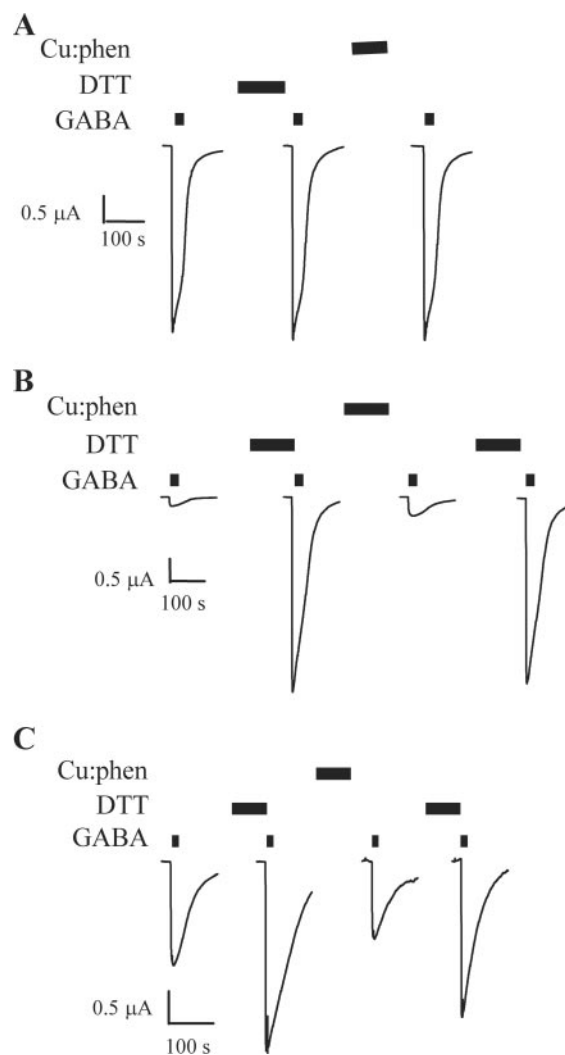


FIG. 2. Disulfide bonds formed in $\alpha 20'C\beta 20'C\gamma 20'C$ and $\alpha \beta 20'C\gamma$, but not wild-type, receptors. The effects of DTT (10 mM, 10 min) and Cu:phen (100:400 μM , 3–6 min) were tested on the maximal GABA-induced current of wild-type (A), $\alpha 20'C\beta 20'C\gamma 20'C$ (B), and $\alpha \beta 20'C\gamma$ (C) receptors. The initial currents of both mutants were smaller than that of wild-type receptors. DTT increased the mutant currents, and subsequent Cu:phen application reversed the effects of DTT. Subsequent DTT application increased currents to an extent comparable to the initial DTT application. Neither reagent significantly altered currents in wild-type receptors. Bars above traces indicate application of reagent. Leak currents have been subtracted. Current is not shown during application of DTT and Cu:phen. Holding potential: -60 mV.

contaminating heavy metals in the buffer, we tested whether the metal chelator EGTA could also potentiate currents in $\alpha 20'C\beta 20'C\gamma 20'C$. DTT potentiated currents by $981 \pm 162\%$, whereas, when applied for several minutes, 1 mM EGTA only potentiated currents by $35 \pm 16\%$ ($n = 3$). Therefore, we conclude that $\alpha 20'C\beta 20'C\gamma 20'C$ formed one or two spontaneous disulfide bonds, which could be reduced by DTT and reformed by Cu:phen.

Disulfide Bond Formation in Receptors with Single 20' Cys Mutant Subunits—Further experiments were aimed at gaining insight into the subunits involved in disulfide bond formation in $\alpha 20'C\beta 20'C\gamma 20'C$. We first examined mutant receptors containing a Cys in only one subunit: $\alpha 20'C\beta\gamma$, $\alpha\beta 20'C\gamma$, and $\alpha\beta\gamma 20'C$. Disulfide bonds formed spontaneously in $\alpha\beta 20'C\gamma$. The initial I_{max} before DTT application, 1078 ± 214 nA ($n = 6$), was smaller than in the wild-type receptors, and after reduction with DTT I_{max} increased to 3251 ± 395 nA ($n = 6$) similar

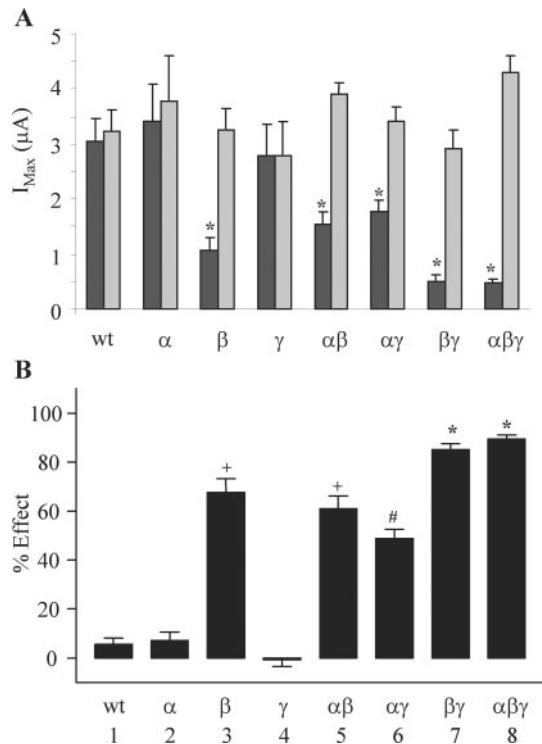


FIG. 3. The effects of disulfide bonds on the GABA-induced currents of 20' cysteine-substitution mutants. *A*, the initial GABA current for all 20' mutants except for $\alpha 20' C \beta \gamma$ and $\alpha \beta \gamma 20' C$ were significantly lower than the wild-type GABA current (*, $p < 0.05$; $n \geq 4$; black bars). Upon reduction with DTT (10 mM, 10 min; gray bars) the GABA current of wild-type and mutant receptors were similar. *B*, the % inhibition produced by disulfide bonds was calculated for all mutants (see text; $n \geq 4$). There were three significantly different groups among those mutants that showed inhibition ($p < 0.05$): $\alpha 20' C \beta \gamma 20' C$ (#), $\alpha \beta 20' C \gamma$ and $\alpha 20' C \beta 20' C \gamma$ (+), and $\alpha \beta 20' C \gamma 20' C$ and $\alpha 20' C \beta 20' C \gamma 20' C$ (*). For each mutant, only subunits containing engineered cysteines are shown. The numbers at the bottom of panel *B* are the bar numbers referred to under "Results."

to wild-type currents (Figs. 2C and 3A). Furthermore, application of 100:400 μ M Cu:phen returned currents to within $3 \pm 23\%$ of the initial untreated levels ($n = 3$), and a second DTT application increased currents to within $33 \pm 5\%$ ($n = 2$) of those after the initial DTT application.

In contrast to $\alpha \beta 20' C \gamma$, in $\alpha 20' C \beta \gamma$ the initial I_{\max} was 3422 ± 664 nA ($n = 4$) comparable to that of wild-type receptors. Application of DTT (3784 ± 813 nA, $n = 4$) or Cu:phen (2655 ± 761 nA, $n = 3$) did not significantly alter GABA I_{\max} from the initial I_{\max} (Fig. 3A). As expected, given that there is only one γ subunit per receptor, there was no evidence for disulfide bond formation in $\alpha \beta \gamma 20' C$ receptors. The initial I_{\max} was 2779 ± 572 nA ($n = 4$). Currents were unaffected by application of either DTT (2791 ± 617 nA, $n = 4$) or Cu:phen (2317 ± 640 nA, $n = 3$) (Fig. 3A). From the experiments on receptors containing a single mutant subunit we conclude that at the 20' position intersubunit disulfide bonds formed between β subunits, but not between α subunits.

Disulfide Bond Formation in Receptors with Two Subunits Containing 20' Cys Mutants—We tested mutants containing Cys in two different subunits for their ability to form disulfide bonds. The initial I_{\max} of $\alpha 20' C \beta \gamma 20' C$, $\alpha 20' C \beta 20' C \gamma$, and $\alpha \beta 20' C \gamma 20' C$ were 1781 ± 209 nA ($n = 10$), 1545 ± 215 nA ($n = 11$), and 567 ± 106 nA ($n = 11$) respectively. All were significantly less than the wild-type receptor I_{\max} . Reduction with DTT increased the currents to levels similar to those of wild type bringing the currents to 3414 ± 265 nA, 3907 ± 195 nA, and 2846 ± 245 nA for $\alpha 20' C \beta \gamma 20' C$, $\alpha 20' C \beta 20' C \gamma$, and

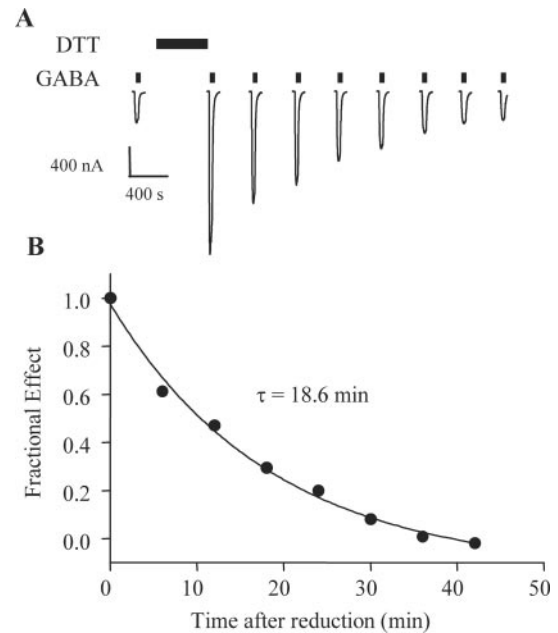


FIG. 4. Measuring the rate of spontaneous disulfide bond formation. *A*, measurement of the rate of spontaneous disulfide bond formation in $\alpha \beta 20' C \gamma 20' C$. After a pulse of 40 μ M GABA, 10 mM DTT was applied for 10 min followed by short pulse of 40 μ M GABA every 6 min. Bars above traces indicate application of reagent. Leak currents have been subtracted. Current not shown during DTT application. *B*, the peak currents from the experiment illustrated in *A* were fitted with a single exponential equation to calculate the τ for disulfide bond formation in $\alpha \beta 20' C \gamma 20' C$. Currents were normalized to the current measured at $t = 0$, and plotted as a function of the time after exposure to DTT.

$\alpha \beta 20' C \gamma 20' C$, respectively (Fig. 3A). Cu:phen reversed the effects of DTT, and a second DTT application duplicated the effects of the first DTT application (data not shown). We conclude that disulfide bonds formed in all three double mutants.

The extent to which disulfide bond formation at the 20' level inhibits GABA-induced currents can be quantified for each mutant using the equation % inhibition = $[(I_{\text{DTT}} - I) / I_{\text{DTT}}] \times 100$, where I and I_{DTT} represent the GABA currents before and after DTT, respectively. Because the currents of untreated receptors (spontaneously oxidized) were of the same magnitude as those of receptors treated with Cu:phen, we used the initial currents in our calculation. The mutants containing a disulfide bond fall into three significantly different groups based on the extent of inhibition (Fig. 3B). Group 1 contains the mutant $\alpha 20' C \beta \gamma 20' C$ with $49 \pm 4\%$ inhibition. Group 2 contains $\alpha \beta 20' C \gamma$ and $\alpha 20' C \beta 20' C \gamma$ with $68 \pm 6\%$ and $61 \pm 5\%$ inhibition, respectively. Group 3 contains $\alpha \beta 20' C \gamma 20' C$ and $\alpha 20' C \beta 20' C \gamma 20' C$ with $81 \pm 3\%$ and $89 \pm 2\%$ inhibition, respectively. From the results above we infer that 1) the two β subunits in a receptor can form a disulfide bond with one another (Fig. 3B, bar #3); 2) the disulfide bond in $\alpha 20' C \beta \gamma 20' C$ must be between an α and a γ subunit (Fig. 3B, bar #6), because a disulfide bond does not form in either of the single mutants $\alpha 20' C \beta \gamma$ or $\alpha \beta \gamma 20' C$ (Fig. 3B, bars #2 and #4); and 3) some portion of the disulfide bonds found in $\alpha \beta 20' C \gamma 20' C$ must be between a β and a γ subunit, because there is more inhibition in the double mutant than the single β mutant (Fig. 3B, compare bars #3 and #7).

The Rate of Disulfide Bond Formation Is Fastest in $\alpha 20' C \beta 20' C \gamma$ —To learn more about the relative proximity and mobility of the different subunits around the channel, we measured the rates of spontaneous disulfide bond formation in $\alpha 20' C \beta 20' C \gamma$, $\alpha 20' C \beta \gamma 20' C$, $\alpha \beta 20' C \gamma 20' C$, and $\alpha \beta 20' C \gamma$. As shown for $\alpha \beta 20' C \gamma 20' C$ in Fig. 4A, a test pulse of GABA was

followed by a 10-min application of 10 mM DTT. Pulses of GABA were then applied every 5–10 min, depending on the mutant. Over the course of several minutes the currents returned to their initial values, indicating the spontaneous reformation of the disulfide bonds. The peak currents of all the pulses were fit with the single exponential equation (Fig. 4B). The τ values for the mutants were as follows ($n \geq 4$): $\alpha 20' C \beta 20' C \gamma$, 3 ± 1 min; $\alpha 20' C \beta \gamma 20' C$, 23 ± 7 min; $\alpha \beta 20' C \gamma 20' C$, 15 ± 2 min; and $\alpha \beta 20' C \gamma$, 17 ± 4 min. $\alpha 20' C \beta 20' C \gamma$ is the only mutant to have a τ significantly different from the other mutants. The difference in disulfide bond formation rates between $\alpha 20' C \beta 20' C \gamma$ and $\alpha \beta 20' C \gamma$ implies that at least some of the disulfide bonds in $\alpha 20' C \beta 20' C \gamma$ are between Cys in α and β subunits. This implies a higher collision rate between the α and β Cys than between the non-adjacent β Cys in $\alpha \beta 20' C \gamma$. This faster rate may be due to disulfide bond formation between adjacent α and β subunits.

$\alpha \beta 20' C \gamma$ Forms a High Affinity, Zn^{2+} -binding Site—The intersubunit disulfide bond that forms between $\beta 20' C$ ys in $\alpha \beta 20' C \gamma$ receptors indicates that the combined movement of the two non-adjacent β M2 segments was sufficient to traverse the channel diameter. The frequency of this event is unknown, because disulfide bonds can trap the receptor in a rare conformation. To address this issue we sought to determine whether these Cys could form a high affinity Zn^{2+} -binding site. Due to the significantly lower energy involved in the Zn^{2+} -Cys interaction compared with a covalent disulfide bond, Zn^{2+} would be unable to trap the rare conformations that could be trapped with a disulfide bond. These experiments were carried out with reduced receptors to ensure that the Cys were fully available to bind Zn^{2+} . In addition, the buffer contained heavy metal chelators to remove any trace metals that might compete with Zn^{2+} for binding to the Cys.

100 μM Zn^{2+} inhibited wild-type $\alpha \beta \gamma$ receptors by $7 \pm 6\%$ ($n = 3$). In contrast, in $\alpha \beta 20' C \gamma$ receptors, 10 μM Zn^{2+} inhibited $96 \pm 1\%$ of the current. The Zn^{2+} IC_{50} for $\alpha \beta 20' C \gamma$ was 34 ± 5 nM ($n = 3$; Fig. 5, A and B), several orders of magnitude smaller than the wild-type $\alpha \beta \gamma$ IC_{50} . In wild-type $\alpha \beta$ receptors, the $\beta 17'$ histidine, $\beta H267$, from adjacent subunits forms a high affinity bidentate Zn^{2+} -binding site (10). To determine whether $\beta H17'$ participated in the formation of an intrasubunit Zn^{2+} -binding site with $\beta 20' C$, we constructed the double mutant, $\beta E20' C / H17' S$ and expressed it with wild-type α and γ subunits. The Zn^{2+} IC_{50} values of $\alpha \beta E20' C / H17' S \gamma$ and $\alpha \beta 20' C \gamma$ were comparable (data not shown). We conclude that Zn^{2+} inhibition of $\alpha \beta 20' C \gamma$ was due to Zn^{2+} binding to an intersubunit, bidentate, Zn^{2+} -binding site formed between the engineered Cys in the two non-adjacent β subunits.

$\alpha 20' C \beta \gamma$ receptors also showed some increased sensitivity to Zn^{2+} compared with wild-type receptors ($n = 4$; Fig. 5B). However, because the predicted IC_{50} would be greater than 100 μM a complete Zn^{2+} dose-response relationship was not determined. The increase over wild-type sensitivity was abolished if, in addition to adding a Cys at $\alpha 20'$, the glutamate at the $\beta 20'$ position was replaced with an asparagine: 100 μM Zn^{2+} inhibited GABA-induced currents in $\alpha 20' C \beta \gamma$ by $32 \pm 4\%$ ($n = 4$), but only altered the $\alpha 20' C \beta 20' N \gamma$ currents by $1 \pm 2\%$ ($n = 3$). Therefore, in $\alpha 20' C \beta \gamma$, a low affinity, bidentate, Zn^{2+} -binding site formed at the 20' position between the engineered cysteine in the α subunit and the native glutamate in the β subunit, but not solely between $\alpha 20'$ Cys.

An Intersubunit Disulfide Bond Does Not Form in $\alpha \beta 17' C \gamma$ —The 17' position is one α helical turn down from the 20' position. Because the distance across the channel between 17' residues should be shorter than it is between 20' residues (13), we tested the ability of $\alpha \beta 17' C \gamma$ to form a disulfide bond.

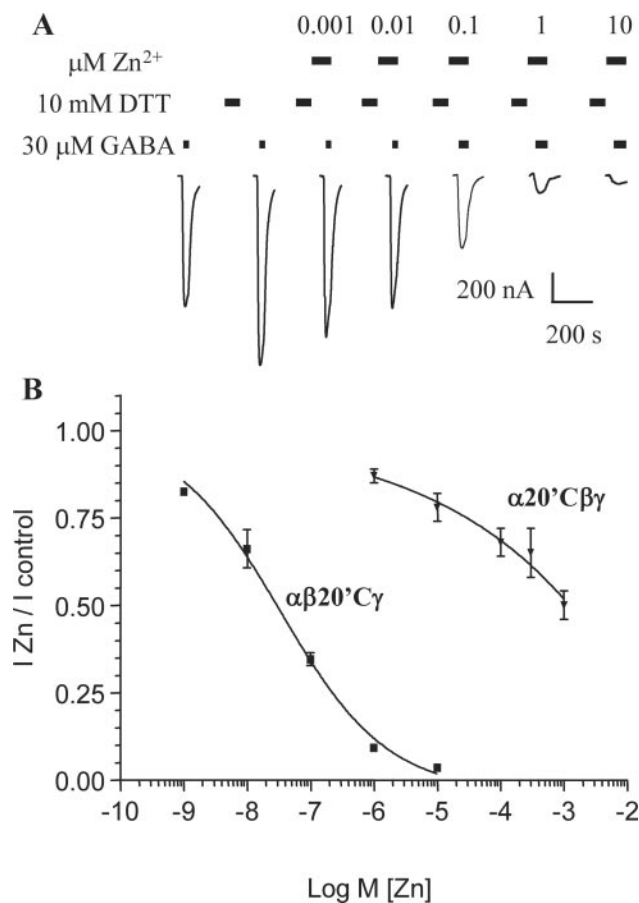


FIG. 5. The engineered cysteines in $\alpha \beta 20' C \gamma$ form a high affinity, bidentate Zn^{2+} -binding site. A, receptors were exposed to increasing Zn^{2+} concentrations. Prior to every pulse of GABA or GABA plus Zn^{2+} , receptors were reduced with DTT (10 mM, 5 min) and either washed or treated with Zn^{2+} for 1 min. A pulse of 30 μM GABA was then applied in the presence of Zn^{2+} . All experiments were done in the presence of metal chelators (see "Experimental Procedures"). Bars above traces indicate application of reagent. Leak currents have been subtracted. Current is not shown during application of Zn^{2+} alone or DTT. Holding potential: -60 mV. B, Zn^{2+} dose-response curves for $\alpha 20' C \beta \gamma$ (triangles) and $\alpha \beta 20' C \gamma$ (squares). Data were normalized to the current in the absence of Zn^{2+} and plotted against the Zn^{2+} concentration. The IC_{50} for $\alpha \beta 20' C \gamma$ was determined by fitting the dose-response curve with the Hill equation (line). A fit for $\alpha 20' C \beta \gamma$ was performed to obtain a partial curve.

DTT and Cu:phen had no effects on maximal GABA-induced currents in $\alpha \beta 17' C \gamma$ (DTT: $+6 \pm 2\%$, $n = 3$; Cu:phen: $-6 \pm 3\%$, $n = 3$). Receptors were also unaffected by DTT using an EC_{10} concentration of GABA, which is more sensitive to modifications that affect gating (wild-type: $+46 \pm 1\%$ ($n = 2$); mutant: $+19 \pm 6\%$ ($n = 3$)). Thus, it appears that β - β disulfide bonds do not form between non-adjacent β subunits at the 17' position in $\alpha \beta \gamma$ receptors.

DISCUSSION

We used disulfide trapping and Zn^{2+} binding to study the mobility of the GABA_A receptor M2 segments in $\alpha \beta \gamma$ receptors. In these receptors there are two α , two β , and one γ subunits. The two α subunits are in non-adjacent positions around the channel axis as are the β subunits (7–11). Our experiments showed that disulfide bonds formed between Cys residues substituted for β_1 Glu-270 (20') but not between Cys substituted for the aligned α_1 subunit residue α_1 Asn-275 (20'). Disulfide bond formation between the engineered β Cys implies that the collision frequency between the engineered $\beta 20'$ Cys is significantly higher than between the α engineered 20' Cys. In the

ACh receptor 4-Å structure the 20' residues have a similar orientation to and distance from the channel axis (13), suggesting that these are not the bases for the disparity between α and β . Thus, at this level in the channel the β subunit M2 segments must be more mobile and/or more flexible than the α subunit M2 segments in $\alpha\beta\gamma$ receptors. This implies that the β M2 segments are less tightly packed with the rest of the protein than the α M2 segments (43, 21).

In the ACh receptor 4-Å structure the α carbons of non-adjacent 20' residues are ~ 19 Å apart (Fig. 6) (13). Because disulfide trapping involves formation of a covalent bond, it does not provide information on the energetics of bringing the 20' residues to within ~ 5 Å necessary to form the disulfide bond. High affinity Zn^{2+} binding involves a non-covalent interaction with pairs of engineered Cys residues. The α carbon separation of the two Cys residues is comparable in a bidentate Zn^{2+} -binding site and in a disulfide bond (29, 44–47). However, unlike disulfide bonds, the energetics of apposing two Cys residues can be measured through the affinity of the resultant binding site for Zn^{2+} . The higher the Zn^{2+} affinity the lower the energy barrier to bringing the two Cys residues close enough to form a bidentate-binding site. Bound Zn^{2+} ions usually display tetrahedral coordination (44, 47, 48). The affinity of a site for Zn^{2+} depends on the number of chelating Cys residues. The Zn^{2+} affinity of sites containing a single Cys residue is generally in the tens of micromolar to millimolar concentration range (29, 31, 49), whereas the Zn^{2+} affinity of proteins containing four Cys residues chelating a Zn^{2+} ion range from 10^{-18} to 10^{-12} M (38, 50–52). The Zn^{2+} affinity for $\beta_1\text{E}20'\text{C}$ containing receptors was 34 nM. To achieve this affinity the Zn^{2+} must be bound by both Cys.

It is difficult to know what the theoretical maximum affinity of two ideally positioned Cys residues is for Zn^{2+} in part because there are no structural Zn^{2+} -binding sites with just two Cys ligands. With this number we could calculate the amount of energy lost to protein distortion by Zn^{2+} binding to the $\beta 20'\text{Cys}$ receptors to give the measured affinity of 34 nM. In proteins containing two Cys residues the Zn^{2+} affinity ranges from nanomolar to micromolar (10, 36, 38). Thus, the 34 nM affinity that we have measured is toward the higher end of measured affinities for two Cys binding. This implies that there is a relatively small energy barrier to bringing the two β Cys from their 19-Å separation distance in the ACh receptor structure to the optimal separation for Zn^{2+} binding.

Disulfide Bonds between α - β , α - γ , and β - γ 20' Cys Mutants—Although the $\alpha 20'\text{C}\beta\gamma$ mutant did not form an intersubunit disulfide bond, the $\alpha 20'\text{Cys}$ was able to form disulfide bonds with the $\beta 20'\text{Cys}$ and with the $\gamma 20'\text{Cys}$. We infer the formation of these α - β and α - γ disulfide bonds, because the extent of inhibition following oxidation was different in the double Cys mutant $\alpha 20'\text{C}\beta 20'\text{C}\gamma$ than in the single Cys mutant $\alpha\beta 20'\text{C}\gamma$ and there was disulfide bond formation in $\alpha 20'\text{C}\beta\gamma 20'\text{C}$ (Fig. 3). In both cases the disulfide bonds could form either between adjacent or between non-adjacent subunits. At present we cannot distinguish between these possibilities. If the disulfide bonds form between $\alpha 20'\text{Cys}$ and a Cys in an adjacent β or γ subunit the M2 segments to which the residues are attached would need to both rotate and move ~ 7 Å based on the ACh receptor structure (Fig. 6). Therefore, while the $\alpha\text{M}2$ 20' region, in conjunction with the $\beta\text{M}2$ or $\gamma\text{M}2$ regions, is sufficiently flexible to move the 7 Å necessary to disulfide bond with a Cys on an adjacent subunit, the 14 Å required for disulfide bonding with a non-adjacent subunit, *i.e.* the other α subunit, appears to be too great a distance for the $\alpha\text{M}2$ segments to overcome.

Gating and Spontaneous Protein Movement—The mobility of the extracellular ends of M2 that we have detected may be

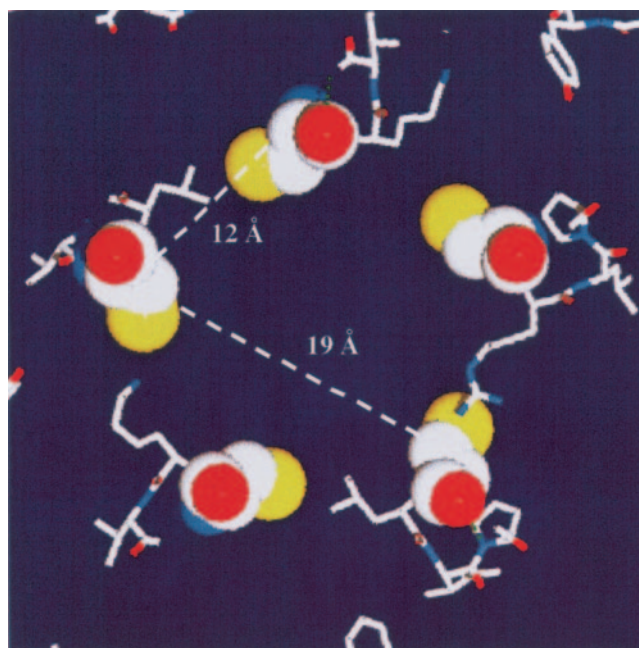


FIG. 6. Model of the M2 segments 20' position illustrating distances between adjacent and non-adjacent subunits. Slab view (5-Å thickness) of the 20' positions, based on the 1OED Protein Data Bank coordinate file for the 4-Å resolution structure of the ACh receptor (13). Native residues have been replaced with cysteines. The van der Waals surfaces are only shown for the cysteines (yellow, sulfur; red, oxygen; blue, nitrogen; and white, carbon). The dotted lines show the α carbon center-to-center distances between adjacent (12 Å) and non-adjacent (19 Å) subunits. To form a disulfide bond or a high affinity Zn^{2+} -binding site the α carbons must approach to within ~ 5 –6 Å.

related to the channel gating process. In the 4-Å ACh receptor structure the channel gate is in the region between the 9' and 14' levels (13). Transduction of agonist binding in the extracellular domain to the gate may proceed through the extracellular end of M2. The strong inhibitory effect of a single disulfide bond at the 20' position ranging from 49% inhibition in $\alpha 20'\text{C}\beta\gamma 20'\text{C}$ to 81% inhibition for $\alpha\beta 20'\text{C}\gamma 20'\text{C}$ demonstrates the importance of this region in channel gating. The motion that we have detected may represent the unsynchronized fluctuation of the extracellular ends of the M2 segments between their closed and open state conformations. Channel opening would require the concerted movement of all five M2 segments away from the channel axis into their open state conformation, an event that rarely occurs in the absence of agonist. The movement of the M2 segments may be similar to the spontaneous conformational fluctuations that the voltage sensing S4 segments undergoes in voltage-dependent K^+ channels as they sense the membrane potential on the two sides of the membrane (53–55).

Our observations of asymmetric motion in the β and α subunits raises the question of whether channel gating involves a larger movement of the β subunit M2 segments than of the α M2 segments. The GABA_A β subunits form the principle portion of the agonist-binding sites, analogous to the ACh receptor α subunits (7). A greater fraction of the agonist surface area interacts with the principle subunit-binding site (7, 56). Whether this causes a greater movement in the β M2 segment is unknown. Differences in the potential coupling of the β and α extracellular domains to the membrane-spanning domains have been observed (57, 58). Whether these differences relate to the extent of M2 segment movement during gating is unknown at present. Perhaps consistent with our finding of greater conformational change in the principle subunit, Unwin and colleagues (59), based on differences between the extracellular domain structure of the *Torpedo* ACh receptor, which is

probably in the closed state, and acetylcholine binding protein (AChBP), which is probably in the activated state, have suggested that agonist binding causes a larger shift in the ACh α subunit structure.

In the region of the gate in the 4-Å structure, the M2 domains from the different subunits appear to make close contact with one another. Specifically, hydrophobic side chains from the 9' to the 14' positions interact to form "a tight hydrophobic girdle around the pore" (13). This girdle, which should impede the mobility of the individual M2 domains, may explain why, at the more proximal 17' position, the β M2 α -helix is less mobile than at the more distal 20' position. The constriction at the central portion of the channel may also help to explain why, in a previous study, no disulfide bonds formed between aligned residues from the 17' to the 6' positions.

The mobility that we have demonstrated in the 20' region with disulfide linkage is also consistent with the results of studies with unnatural amino acids. Using α -hydroxy acids in place of amino acids they converted the backbone peptide amide to an ester linkage. They inferred that there was more backbone conformational changes in the extracellular half of the ACh receptor M2 segment (20). Using linear free energy relationship analysis, it has also been shown that the extracellular half of M2 appears to move as a unit in the ACh-induced gating process (2, 60).

The range of motion that we have inferred for the β subunit M2 α -helices is not without precedent. In a study of protein backbone flexibility in the *Escherichia coli* D-galactose chemosensory receptor, a protein of known crystal structure, Falke and colleagues found two cysteines that could traverse 15 Å to form a disulfide bond (28, 61, 62). The time constant for the formation of this disulfide bond in the chemosensory receptor mutant was 3630 s in the presence of 1.5:4.5 mM Cu:phen, more than ten times slower than the formation time constant in $\alpha\beta$ 20'C γ , where disulfide formation went to completion within 360 s in the presence of 100:400 μ M Cu:phen (data not shown). The difference in the formation rates are probably even greater because in the chemosensory receptor experiments the Cu:phen concentration was over 10 times higher and the temperature was 12–15 degrees higher (37 °C and 25 °C for the chemosensory and GABA_A receptors, respectively). Extrapolating from the results of Careaga and Falke (28), the collision rate between the engineered β 20' Cys must be at least 10^3 s⁻¹ and is probably higher, because their experiments were performed under significantly more oxidizing conditions than ours. In the bacterial mechanosensitive channel MscL state-dependent disulfide bond formation occurs between engineered Cys residues that are separated by >10 Å in the crystal structure. Disulfide bond formation between the MscL V15C required 1 mM Cu:phen and took about 30 min to go to completion (63). This suggests a lower collision frequency in MscL V15C than we observed for the GABA_A receptor β 20' Cys in the present study.

Alternative Interpretations—Although we believe that the above interpretation of our data is most likely, it rests on the structural foundation provided by the 4-Å resolution ACh receptor structure. An alternative interpretation that we believe is unlikely but that we cannot exclude is that our data suggest that the closed-state structure of the GABA_A receptor is different than the published ACh receptor structure (13). The ability to form disulfide bonds and a high affinity Zn²⁺-binding site only between the β 20'Cys may indicate there is a significant structural asymmetry at the 20' level such that the average separation of the β 20' residues is smaller than the α 20' residues.

CONCLUSION

We have shown that, at the 20' level in the GABA_A receptor M2 segments, a disulfide bond or a high affinity Zn²⁺-binding site can form between engineered Cys residues in the β subunits. In contrast, an engineered Cys at the aligned position in the α subunits forms neither. Based on the roughly symmetrical positions of the aligned residues relative to the channel axis in the 4-Å ACh receptor structure, we infer that the extracellular ends of the β M2 segments are more mobile than the α M2 segments. The increased mobility is likely due to looser protein packing around the β M2 segments. In the ACh receptor structure the α carbon atoms of the non-adjacent 20' residues are separated by ~19 Å. Thus, together the two β 20'Cys must move ~14 Å to form a disulfide bond or each must move about 7 Å toward the central axis. A similar amount of translational movement would be necessary to bring the two Cys into close proximity to form a Zn²⁺-binding site. Given the high affinity with which Zn²⁺ was bound by the two β 20'Cys, we infer that there must be a low energy barrier to this movement. This suggests that there is a relatively flat potential energy surface for the movement of the β M2 segments. These experiments begin to provide information on the dynamic movement of the channel-lining M2 segments and complement the static picture of the channel structure that is obtained from the cryo-EM structure of the homologous ACh receptor.

Acknowledgments—We thank Maya Chatav and Rachel Berkowitz for expert technical assistance; Pierre Paoletti (Ecole Normale Supérieure, France) for advice on the use of heavy metal chelators to buffer Zn²⁺ concentrations; Sara Nunez for discussions on the energetics of Zn²⁺ binding; and Moez Bali, Amal Bera, Maria Gulino, David Liebelt, Michaela Jansen, and David Reeves for helpful discussions and for comments on the manuscript.

REFERENCES

- Moss, S. J., and Smart, T. G. (2001) *Nat. Rev. Neurosci.* **2**, 240–250
- Auerbach, A. (2003) *Science's STKE* <http://stke.sciencemag.org/cgi/content/full/sigtrans;2003/188/re11>
- Whiting, P. J. (2003) *Curr. Opin. Drug Discov. Dev.* **6**, 648–657
- Karlin, A., and Akabas, M. H. (1995) *Neuron* **15**, 1231–1244
- Hevers, W., and Luddens, H. (1998) *Mol. Neurobiol.* **18**, 35–86
- Lester, H. A., Dibas, M. I., Dahan, D. S., Leite, J. F., and Dougherty, D. A. (2004) *Trends Neurosci.* **27**, 329–336
- Brejč, K., van Dijk, W. J., Klaassen, R. V., Schuurmans, M., van Der Oost, J., Smit, A. B., and Sixma, T. K. (2001) *Nature* **411**, 269–276
- Cromer, B. A., Morton, C. J., and Parker, M. W. (2002) *Trends Biochem. Sci.* **27**, 280–287
- Tretter, V., Ehya, N., Fuchs, K., and Sieghart, W. (1997) *J. Neurosci.* **17**, 2728–2737
- Horenstein, J., and Akabas, M. H. (1998) *Mol. Pharmacol.* **53**, 870–877
- Baumann, S. W., Baur, R., and Sigel, E. (2001) *J. Biol. Chem.* **276**, 36275–36280
- Xu, M., and Akabas, M. H. (1996) *J. Gen. Physiol.* **107**, 195–205
- Miyazawa, A., Fujiyoshi, Y., and Unwin, N. (2003) *Nature* **423**, 949–955
- Miller, C. (1989) *Neuron* **2**, 1195–1205
- Imoto, K., Busch, C., Sakmann, B., Mishina, M., Konno, T., Nakai, J., Bujo, H., Mori, Y., Fukuda, K., and Numa, S. (1988) *Nature* **335**, 645–648
- Le Novère, N., Corringer, P. J., and Changeux, J. P. (1999) *Biophys. J.* **76**, 2329–2345
- Bera, A. K., Chatav, M., and Akabas, M. H. (2002) *J. Biol. Chem.* **277**, 43002–43010
- Wilson, G. G., and Karlin, A. (1998) *Neuron* **20**, 1269–1281
- Panicker, S., Cruz, H., Arrabit, C., and Slesinger, P. A. (2002) *J. Neurosci.* **22**, 1629–1639
- England, P. M., Zhang, Y., Dougherty, D. A., and Lester, H. A. (1999) *Cell* **96**, 89–98
- Goren, E. N., Reeves, D. C., and Akabas, M. H. (2004) *J. Biol. Chem.* **279**, 11198–11205
- Panicker, S., Cruz, H., Arrabit, C., Suen, K. F., and Slesinger, P. A. (2004) *J. Biol. Chem.* **279**, 28149–28158
- Villarroel, A., Herlitze, S., Koenen, M., and Sakmann, B. (1991) *Proc. R. Soc. Lond. B. Biol. Sci.* **243**, 69–74
- Galzi, J. L., Devillers-Thiery, A., Hussy, N., Bertrand, S., Changeux, J. P., and Bertrand, D. (1992) *Nature* **359**, 500–505
- Akabas, M. H., Kaufmann, C., Archdeacon, P., and Karlin, A. (1994) *Neuron* **13**, 919–927
- Horenstein, J., Wagner, D. A., Czajkowski, C., and Akabas, M. H. (2001) *Nat. Neurosci.* **4**, 477–485
- Kobashi, K. (1968) *Biochim. Biophys. Acta* **158**, 239–245
- Careaga, C. L., and Falke, J. J. (1992) *J. Mol. Biol.* **226**, 1219–1235
- Berg, J. M., and Shi, Y. (1996) *Science* **271**, 1081–1085
- Higaki, J. H., Fletterick, R. J., and Craik, C. S. (1992) *Trends Biochem. Sci.* **17**,

- 100–104
31. Regan, L. (1995) *Trends Biochem. Sci.* **20**, 280–285
32. Regan, L., Rockwell, A., Wasserman, Z., and DeGrado, W. (1994) *Protein Sci.* **3**, 2419–2427
33. Yu, H., Kono, M., McKee, T. D., and Oprian, D. D. (1995) *Biochemistry* **34**, 14963–14969
34. Wu, J., and Kaback, H. R. (1996) *Proc. Natl. Acad. Sci. U. S. A.* **93**, 14498–14502
35. Holmgren, M., Shin, K. S., and Yellen, G. (1998) *Neuron* **21**, 617–621
36. Gether, U., Norregaard, L., and Loland, C. J. (2001) *Life Sci.* **68**, 2187–2198
37. Hosié, A. M., Dunne, E. L., Harvey, R. J., and Smart, T. G. (2003) *Nat. Neurosci.* **6**, 362–369
38. Paoletti, P., Ascher, P., and Neyton, J. (1997) *J. Neurosci.* **17**, 5711–5725
39. Fayyazuddin, A., Villarroel, A., Le Goff, A., Lerma, J., and Neyton, J. (2000) *Neuron* **25**, 683–694
40. Pritchett, D. B., Sontheimer, H., Shivers, B. D., Ymer, S., Kettenmann, H., Schofield, P. R., and Seeburg, P. H. (1989) *Nature* **338**, 582–585
41. Boileau, A. J., Kucken, A. M., Evers, A. R., and Czajkowski, C. (1998) *Mol. Pharmacol.* **53**, 295–303
42. Woollorton, J. R., McDonald, B. J., Moss, S. J., and Smart, T. G. (1997) *J. Physiol. (Lond.)* **505**, 633–640
43. Halle, B. (2002) *Proc. Natl. Acad. Sci. U. S. A.* **99**, 1274–1279
44. Christianson, D. W. (1991) *Adv. Protein Chem.* **42**, 281–355
45. Regan, L. (1993) *Annu. Rev. Biophys. Biomol. Struct.* **22**, 257–287
46. Krovetz, H. S., VanDongen, H. M., and VanDongen, A. M. (1997) *Biophys. J.* **72**, 117–126
47. Alberts, I. L., Nadassy, K., and Wodak, S. J. (1998) *Prot. Sci.* **7**, 1700–1716
48. Auld, D. S. (2001) *Biometals* **14**, 271–313
49. Dolinska, B. (2001) *Farmacologia* **56**, 737–740
50. Choi, Y., Chen, H. V., and Lipton, S. A. (2001) *J. Neurosci.* **21**, 392–400
51. Pabo, C. O., Peisach, E., and Grant, R. A. (2001) *Annu. Rev. Biochem.* **70**, 313–340
52. Collet, J. F., D'Souza, J. C., Jakob, U., and Bardwell, J. C. (2003) *J. Biol. Chem.* **278**, 45325–45332
53. Starace, D. M., Stefani, E., and Bezanilla, F. (1997) *Neuron* **19**, 1319–1327
54. Starace, D. M., and Bezanilla, F. (2001) *J. Gen. Physiol.* **117**, 469–490
55. Jiang, Y., Lee, A., Chen, J., Ruta, V., Cadene, M., Chait, B. T., and MacKinnon, R. (2003) *Nature* **423**, 33–41
56. Celie, P. H., van Rossum-Fikkert, S. E., van Dijk, W. J., Brejc, K., Smit, A. B., and Sixma, T. K. (2004) *Neuron* **41**, 907–914
57. Kash, T. L., Jenkins, A., Kelley, J. C., Trudell, J. R., and Harrison, N. L. (2003) *Nature* **421**, 272–275
58. Kash, T. L., Dizon, M. J., Trudell, J. R., and Harrison, N. L. (2004) *J. Biol. Chem.* **279**, 4887–4893
59. Unwin, N., Miyazawa, A., Li, J., and Fujiyoshi, Y. (2002) *J. Mol. Biol.* **319**, 1165–1176
60. Cymes, G. D., Grosman, C., and Auerbach, A. (2002) *Biochemistry* **41**, 5548–5555
61. Careaga, C. L., Sutherland, J., Sabeti, J., and Falke, J. J. (1995) *Biochemistry* **34**, 3048–3055
62. Danielson, M. A., Bass, R. B., and Falke, J. J. (1997) *J. Biol. Chem.* **272**, 32878–32888
63. Shapovalov, G., Bass, R., Rees, D. C., and Lester, H. A. (2003) *Biophys. J.* **84**, 2357–2365